PERGAMON

International Journal of Solids and Structures 38 (2001) 4969–4985

INTERNATIONAL JOURNAL OF SOLIDS and STRUCTURES

www.elsevier.com/locate/ijsolstr

A general plane-stress solution in cylindrical coordinates for a piezothermoelastic plate

Fumihiro Ashida [a], Theodore R. Tauchert [b,*]

[a] *Department of Electronic and Control Systems Engineering, Shimane University, Matsue, Shimane 690-8504, Japan*
[b] *Department of Mechanical Engineering, University of Kentucky, Lexington, KY 40506-0046, USA*

Received 24 March 2000

Abstract

A general solution procedure is proposed for plane-stress problems of circular plates constructed from piezothermoelastic material. Potential functions are introduced in order to uncouple the equations governing equilibrium and electrostatics. The present formulation is applicable to plates having arbitrary edge conditions. Solutions are derived for plates having either radially constrained or traction-free edges and subjected to axisymmetric surface heating. Numerical results illustrate the effects of plate thickness and variations in material properties upon the induced elastic displacements, stresses, electric potential and electric displacements.

Keywords: Plane-stress; Circular plate; Piezothermoelastic; Surface heating; Potential functions

1. Introduction

Increased interest in piezothermoelasticity during recent years can be attributed to the fact that piezoelectric materials have potential for use in intelligent structural systems, including systems designed to operate in thermal environments. The coupling that exists between the thermal/elastic/electric fields in piezoelectric bodies provides a mechanism for sensing and controlling thermomechanical deformation. In order for the potential of piezoelectric-based intelligent structures to be fully realized, further research is needed.

Investigations that have dealt with the response of plates constructed of piezoelastic materials include applications based upon classical (Lee, 1990), first-order (Chandrashekhara and Agarwal, 1993), and higher-order (Ray et al., 1993a; Mitchell and Reddy, 1995; Saravanos et al., 1997; etc.) deformation theories. Exact solutions for simply-supported hybrid laminates containing piezoelectric layers have been presented by Ray et al. (1993b) and Heyliger (1994).

In addition to the aforementioned investigations that considered isothermal conditions, a number of studies have addressed thermoelectroelastic plate response. Equations governing linear piezothermoelastic

* Corresponding author. Tel.: +1-859-257-2629; fax: +1-859-257-8057.
E-mail address: tauchert@engr.uky.edu (T.R. Tauchert).

0020-7683/01/$ - see front matter
PII: S0020-7683(00)00321-8

behavior were presented first by Mindlin (1961). Tiersten (1971) derived a general nonlinear theory of thermoelectroelasticity. In recent years the response of piezothermoelastic plates to thermal loading has been analyzed on the basis of classical (Tauchert, 1992; Noda and Kimura, 1998), first-order (Jonnalagadda et al., 1994), higher-order (Reddy, 1996; Tang et al., 1996; etc.), and exact three-dimensional (Xu et al., 1995; Dube et al., 1996; Kapuria et al., 1998) formulations. A review of these and other recent developments in this area, particularly those related to smart composite structures, was presented by Tauchert et al. (2000).

As an alternative to two-dimensional plate theories based upon simplifying assumptions regarding through-thickness distributions of displacements, a plane-stress formulation was considered by Ashida and Tauchert (2000). They derived an exact solution to the plane problem of a circular piezothermoelastic plate constrained against radial deformation and subjected to axisymmetric heating, and compared the plane-stress results with those based on an exact three-dimensional solution (Ashida and Tauchert, 1998). The present paper extends the earlier investigation by providing a general solution procedure for plane-stress problems of a circular piezothermoelastic plate having arbitrary edge conditions and subject to thermal surface loading. Numerical results for traction-free plates are presented.

2. Governing equations

We consider the response of a piezothermoelastic solid possessing hexagonal material symmetry of class 6mm. Constitutive equations for the stresses σ_{ij}, expressed in cylindrical coordinates, are

$$\begin{aligned}
\sigma_{rr} &= c_{11}\varepsilon_{rr} + c_{12}\varepsilon_{\theta\theta} + c_{13}\varepsilon_{zz} - e_1 E_z - \beta_1 T \\
\sigma_{\theta\theta} &= c_{12}\varepsilon_{rr} + c_{11}\varepsilon_{\theta\theta} + c_{13}\varepsilon_{zz} - e_1 E_z - \beta_1 T \\
\sigma_{zz} &= c_{13}\varepsilon_{rr} + c_{13}\varepsilon_{\theta\theta} + c_{33}\varepsilon_{zz} - e_3 E_z - \beta_3 T \\
\sigma_{\theta z} &= c_{44}\varepsilon_{\theta z} - e_4 E_\theta \\
\sigma_{zr} &= c_{44}\varepsilon_{zr} - e_4 E_r \\
\sigma_{r\theta} &= (c_{11} - c_{12})\varepsilon_{r\theta}/2
\end{aligned} \tag{1}$$

where ε_{ij} are the strain components, E_i are the electric field intensities, T denotes the temperature rise, c_{ij} are elastic stiffnesses, e_i are stress-piezoelectric constants, and β_i are stress-temperature coefficients. The strains ε_{ij} are related to the displacements u_i by

$$\begin{aligned}
&\varepsilon_{rr} = u_{r,r}, \qquad \varepsilon_{\theta\theta} = \frac{1}{r}u_r + \frac{1}{r}u_{\theta,\theta}, \qquad \varepsilon_{zz} = u_{z,z} \\
&\varepsilon_{\theta z} = u_{\theta,z} + \frac{1}{r}u_{z,\theta}, \qquad \varepsilon_{zr} = u_{z,r} + u_{r,z}, \qquad \varepsilon_{r\theta} = \frac{1}{r}u_{r,\theta} + u_{\theta,r} - \frac{1}{r}u_\theta.
\end{aligned} \tag{2}$$

The constitutive relations for the electric field are

$$\begin{aligned}
D_r &= e_4\varepsilon_{zr} + \eta_1 E_r \\
D_\theta &= e_4\varepsilon_{\theta z} + \eta_1 E_\theta \\
D_z &= e_1\varepsilon_{rr} + e_1\varepsilon_{\theta\theta} + e_3\varepsilon_{zz} + \eta_3 E_z + p_3 T
\end{aligned} \tag{3}$$

where D_i are the electric displacement components, η_i are dielectric permittivities, and p_3 is the pyroelectric constant.

For a state of plane stress perpendicular to the z-axis

$$\sigma_{zz} = \sigma_{\theta z} = \sigma_{zr} = 0 \tag{4}$$

in which case

$$\varepsilon_{zz} = \frac{1}{c_{33}}(-c_{13}\varepsilon_{rr} - c_{13}\varepsilon_{\theta\theta} + e_3 E_z + \beta_3 T), \qquad \varepsilon_{\theta z} = \frac{e_4}{c_{44}} E_\theta, \qquad \varepsilon_{zr} = \frac{e_4}{c_{44}} E_r \tag{5}$$

The equations of equilibrium for the state of plane stress are

$$\begin{aligned} &\sigma_{rr,r} + \frac{\sigma_{r\theta,\theta}}{r} + \frac{\sigma_{rr} - \sigma_{\theta\theta}}{r} = 0 \\ &\sigma_{r\theta,r} + \frac{\sigma_{\theta\theta,\theta}}{r} + \frac{2\sigma_{r\theta}}{r} = 0 \end{aligned} \tag{6}$$

and the equation of electrostatics is

$$D_{r,r} + \frac{D_{\theta,\theta}}{r} + D_{z,z} + \frac{D_r}{r} = 0 \tag{7}$$

The temperature field is governed by Fourier's heat conduction equation

$$T_{,rr} + \frac{1}{r} T_{,r} + \frac{1}{r^2} T_{,\theta\theta} + \lambda^2 T_{,zz} = \frac{T_{,t}}{\kappa} \tag{8}$$

where $\lambda^2 = \lambda_z/\lambda_r$ denotes the ratio of the coefficients of heat conduction in the z and r directions, and κ is thermal diffusivity.

3. General solution technique

A general solution to the plane-stress problem is obtained here by superposition of a piezothermoelastic (particular) solution and a piezoelastic (complementary) solution. The piezothermoelastic solution is based upon two displacement potential functions Ω and Θ and an electric potential χ_1, and the formulation is similar to the less general solution derived earlier by Ashida and Tauchert (2000). The corresponding piezoelastic solution is expressed in terms of a displacement potential ϕ that is analogous to Love's function for isotropic elasticity, and an electric potential χ_2.

3.1. Solution I

In order to obtain a particular solution to Eqs. (6) and (7), the displacement and electric force components are expressed in terms of potential functions Ω, Θ and χ_1 as

$$\begin{aligned} &u_r = \Omega_{,r}, \qquad u_\theta = \frac{\Omega_{,\theta}}{r}, \qquad u_z = \Theta_{,z} \\ &E_r = -\chi_{1,r}, \qquad E_\theta = -\frac{\chi_{1,\theta}}{r}, \qquad E_z = -\chi_{1,z} \end{aligned} \tag{9}$$

The nonzero strains in this case are

$$\varepsilon_{rr} = \Omega_{,rr}, \qquad \varepsilon_{\theta\theta} = \frac{\Omega_{,r}}{r} + \frac{\Omega_{,\theta\theta}}{r^2}, \qquad \varepsilon_{zz} = \Theta_{,zz}, \qquad \varepsilon_{r\theta} = 2\left(\frac{\Omega_{,r\theta}}{r} - \frac{\Omega_{,\theta}}{r^2}\right) \tag{10}$$

and the corresponding stresses become

$$\begin{aligned}
\sigma_{rr} &= c_{11}\Omega_{,rr} + c_{12}\left(\frac{\Omega_{,r}}{r} + \frac{\Omega_{,\theta\theta}}{r^2}\right) + c_{13}\Theta_{,zz} + e_1\chi_{1,z} - \beta_1 T \\
\sigma_{\theta\theta} &= c_{12}\Omega_{,rr} + c_{11}\left(\frac{\Omega_{,r}}{r} + \frac{\Omega_{,\theta\theta}}{r^2}\right) + c_{13}\Theta_{,zz} + e_1\chi_{1,z} - \beta_1 T \\
\sigma_{r\theta} &= (c_{11} - c_{12})\left(\frac{\Omega_{,r\theta}}{r} - \frac{\Omega_{,\theta}}{r^2}\right)
\end{aligned} \tag{11}$$

Substitution of Eq. (11) into Eq. (6) shows that equilibrium is satisfied providing the potential functions Ω, Θ and χ_1 satisfy the relation

$$c_{11}\Delta_1\Omega + c_{13}\Theta_{,zz} = -e_1\chi_{1,z} + \beta_1 T \tag{12}$$

where

$$\Delta_1 = \frac{\partial^2}{\partial r^2} + \frac{1}{r}\frac{\partial}{\partial r} + \frac{1}{r^2}\frac{\partial^2}{\partial\theta^2} \tag{13}$$

The electric displacements are, according to Eqs. (3) and (5),

$$\begin{aligned}
D_r &= -\left(\eta_1 + \frac{e_4^2}{c_{44}}\right)\chi_{1,r}, \qquad D_\theta = -\left(\eta_1 + \frac{e_4^2}{c_{44}}\right)\frac{\chi_{1,\theta}}{r} \\
D_z &= e_1\Delta_1\Omega + e_3\Theta_{,zz} - \eta_3\chi_{1,z} + p_3 T
\end{aligned} \tag{14}$$

Substitution of expressions (14) into the equation of electrostatics (7) yields

$$-\left(\eta_1 + \frac{e_4^2}{c_{44}}\right)\Delta_1\chi_1 - \eta_3\chi_{1,zz} + e_1\Delta_1\Omega_{,z} + e_3\Theta_{,zzz} = -p_3 T_{,z} \tag{15}$$

It follows from Eqs. (5) and (9) that for plane stress

$$\Theta_{,zz} = -\frac{c_{13}}{c_{33}}\Delta_1\Omega - \frac{e_3}{c_{33}}\chi_{1,z} + \frac{\beta_3}{c_{33}}T \tag{16}$$

Eq. (16) can be used to eliminate the potential function Θ from the equilibrium and electrostatics equations (12) and (15); the resulting two equations, together with Eq. (16), can be rearranged and expressed in the following form:

$$\Delta_1\Omega = \delta_1\chi_{1,z} + \xi_2 T \tag{17}$$

$$\Theta_{,zz} = -\delta_2\chi_{1,z} + \xi_3 T \tag{18}$$

$$\Delta_1\chi_1 + \mu^2\chi_{1,zz} = \xi_1 T_{,z} \tag{19}$$

in which

$$\begin{aligned}
\delta_1 &= \frac{c_{13}e_3 - c_{33}e_1}{c_{11}c_{33} - c_{13}^2}, \qquad \delta_2 = \frac{c_{13}\delta_1 + e_3}{c_{33}} \\
\xi_1 &= \frac{c_{44}[(c_{33}p_3 + e_3\beta_3)(c_{11}c_{33} - c_{13}^2) - (c_{13}e_3 - c_{33}e_1)(c_{33}\beta_1 - c_{13}\beta_3)]}{c_{33}(\eta_1 c_{44} + e_4^2)(c_{11}c_{33} - c_{13}^2)} \\
\xi_2 &= \frac{c_{33}\beta_1 - c_{13}\beta_3}{c_{11}c_{33} - c_{13}^2}, \qquad \xi_3 = \frac{\beta_3 - c_{13}\xi_2}{c_{33}} \\
\mu^2 &= \frac{c_{44}[(c_{33}\eta_3 + e_3^2)(c_{11}c_{33} - c_{13}^2) + (c_{13}e_3 - c_{33}e_1)^2]}{c_{33}(\eta_1 c_{44} + e_4^2)(c_{11}c_{33} - c_{13}^2)}
\end{aligned} \tag{20}$$

3.2. Solution II

For a complementary solution to the piezoelastic problem (corresponding to zero thermal loading), the displacement and electric force components are written in terms of potential functions ϕ and χ_2 as

$$\begin{aligned} u_r &= -k_1\phi_{,rz}, \qquad u_\theta = -k_1\frac{\phi_{,\theta z}}{r}, \qquad u_z = k_2\Delta_1\phi \\ E_r &= -\chi_{2,r}, \qquad E_\theta = -\frac{\chi_{2,\theta}}{r}, \qquad E_z = -\chi_{2,z} \end{aligned} \tag{21}$$

The corresponding strains, stresses and electric displacements are

$$\varepsilon_{rr} = -k_1\phi_{,rrz}, \qquad \varepsilon_{\theta\theta} = -k_1\left(\frac{\phi_{,rz}}{r} + \frac{\phi_{,\theta\theta z}}{r^2}\right), \qquad \varepsilon_{zz} = k_2\Delta_1\phi_{,z}, \qquad \varepsilon_{r\theta} = -2k_1\left(\frac{\phi_{,r\theta z}}{r} - \frac{\phi_{,\theta z}}{r^2}\right) \tag{22}$$

and

$$\begin{aligned} \sigma_{rr} &= -k_1c_{11}\phi_{,rrz} - k_1c_{12}\left(\frac{\phi_{,rz}}{r} + \frac{\phi_{,\theta\theta z}}{r^2}\right) + k_2c_{13}\Delta_1\phi_{,z} + e_1\chi_{2,z} \\ \sigma_{\theta\theta} &= -k_1c_{12}\phi_{,rrz} - k_1c_{11}\left(\frac{\phi_{,rz}}{r} + \frac{\phi_{,\theta\theta z}}{r^2}\right) + k_2c_{13}\Delta_1\phi_{,z} + e_1\chi_{2,z} \\ \sigma_{r\theta} &= -k_1(c_{11} - c_{12})\left(\frac{\phi_{,r\theta z}}{r} - \frac{\phi_{,\theta z}}{r^2}\right) \end{aligned} \tag{23}$$

and also

$$D_r = -\left(\eta_1 + \frac{e_4^2}{c_{44}}\right)\chi_{2,r}, \qquad D_\theta = -\left(\eta_1 + \frac{e_4^2}{c_{44}}\right)\frac{\chi_{2,\theta}}{r}, \qquad D_z = (-k_1e_1 + k_2e_3)\Delta_1\phi_{,z} - \eta_3\chi_{2,z} \tag{24}$$

In this case the equations of equilibrium (6) and electrostatics (7) are satisfied providing the potential functions ϕ and χ_2 satisfy the equations

$$\Delta_1(\Delta_1\phi + \mu^2\phi_{,zz}) = 0 \tag{25}$$

$$\chi_2 = -\Delta_1\phi \tag{26}$$

and k_1 and k_2 have the values

$$k_1 = \frac{c_{13}e_3 - c_{33}e_1}{c_{11}c_{33} - c_{13}^2} = \delta_1, \qquad k_2 = \frac{c_{11}e_3 - c_{13}e_1}{c_{11}c_{33} - c_{13}^2} = \delta_2 \tag{27}$$

The general solution for the piezothermoelastic response of the plate is obtained through superposition of solutions I and II; i.e.,

$$\begin{aligned} u_r &= \Omega_{,r} - k_1\phi_{,rz}, \qquad u_\theta = \frac{\Omega_{,\theta}}{r} - k_1\frac{\phi_{,\theta z}}{r}, \qquad u_z = \Theta_{,z} + k_2\Delta_1\phi \\ E_r &= -\Phi_{,r}, \qquad E_\theta = -\frac{\Phi_{,\theta}}{r}, \qquad E_z = -\Phi_{,z} \end{aligned} \tag{28}$$

where the total electric potential is given by

$$\Phi = \chi_1 + \chi_2 \tag{29}$$

4. Application

Next we examine the response of a plate of radius a and depth b, subject to axisymmetric heating on one face, zero temperature rise on the opposite face, and thermal insulation on the cylindrical edge. The thermal boundary conditions in this case are

$$T = 0 \quad \text{on } z = 0 \tag{30}$$

$$T_{,z} + hT = hQ(r) \quad \text{on } z = b \tag{31}$$

$$T_{,r} = 0 \quad \text{on } r = a \tag{32}$$

where h denotes the relative surface heat transfer coefficient, and $Q(r)$ is a prescribed function. The temperature field that satisfies conditions (30)–(32) can be expressed as (Ashida and Tauchert, 2000)

$$T(r,z) = T_0(z) + T_1(r,z) \tag{33}$$

where

$$T_0 = A_0 \frac{z}{b}, \qquad T_1 = \sum_{n=1}^{\infty} A_n J_0(\alpha_n r) \frac{\sinh(\alpha_n z/\lambda)}{\sinh(\alpha_n b/\lambda)} \tag{34}$$

in which

$$A_0 = \frac{hb\overline{Q}_0}{1+hb}, \qquad A_n = \frac{\lambda h \overline{Q}_n}{\lambda h + \alpha_n \coth(\alpha_n b/\lambda)} \tag{35}$$

$$\overline{Q}_0 = \frac{2}{a^2}\int_0^a rQ(r)\,\mathrm{d}r, \qquad \overline{Q}_n = \frac{2}{a^2 J_0^2(\alpha_n a)}\int_0^a rQ(r)J_0(\alpha_n r)\,\mathrm{d}r \tag{36}$$

and α_n are the roots of the equation

$$J_1(\alpha_n a) = 0 \tag{37}$$

The piezothermoelastic response to this temperature field is investigated for two different edge conditions, namely radially constrained (Case A) and traction-free (Case B).

4.1. Case A. Radially constrained edge

Consider first the situation in which the cylindrical edge ($r = a$) of the plate is constrained against radial displacement, and free of electric charge. The top and bottom faces ($z = 0, b$) are also assumed to be electrically charge free. The boundary conditions for this case are expressed as

$$u_r = 0 \quad \text{on } r = a \tag{38}$$

$$D_r = 0 \quad \text{on } r = a \tag{39}$$

$$D_z = 0 \quad \text{on } z = 0, b \tag{40}$$

In the case of the temperature distribution $T_0(z) = A_0(z/b)$ it easily can be shown that the solution to the plane-stress equations of equilibrium and electrostatics, together with boundary conditions (38)–(40), is given by

$$u_r = 0, \qquad u_z = \gamma_1 A_0 \frac{z^2}{2b} \tag{41}$$

$$\sigma_{rr} = \sigma_{\theta\theta} = (c_{13}\gamma_1 + e_1\gamma_2 - \beta_1)A_0\frac{z}{b} \tag{42}$$

$$\Phi = \gamma_2 A_0 \frac{z^2}{2b} \tag{43}$$

$$D_r = D_z = 0 \tag{44}$$

in which

$$\gamma_1 = \frac{\beta_3\eta_3 - e_3p_3}{c_{33}\eta_3 + e_3^2}, \qquad \gamma_2 = \frac{c_{33}p_3 + \beta_3 e_3}{c_{33}\eta_3 + e_3^2} \tag{45}$$

The solution corresponding to the temperature distribution $T_1(r,z)$ given by Eq. (34) is obtained using the potential functions introduced in Section 3. For the piezothermoelastic solution (Solution I), the potential function χ_1 that satisfies Eq. (19) is

$$\chi_1 = \sum_{n=1}^{\infty} D_n J_0(\alpha_n r)\frac{\cosh(\alpha_n z/\lambda)}{\sinh(\alpha_n b/\lambda)} \tag{46}$$

where

$$D_n = \frac{\lambda\xi_1 A_n}{(\mu^2 - \lambda^2)\alpha_n} \tag{47}$$

Then potential functions Ω and Θ satisfying Eqs. (17) and (18), respectively, become

$$\Omega = \sum_{n=1}^{\infty} E_n J_0(\alpha_n r)\frac{\sinh(\alpha_n z/\lambda)}{\sinh(\alpha_n b/\lambda)} \tag{48}$$

$$\Theta = \sum_{n=1}^{\infty} F_n J_0(\alpha_n r)\frac{\sinh(\alpha_n z/\lambda)}{\sinh(\alpha_n b/\lambda)} \tag{49}$$

where

$$E_n = -\frac{1}{\alpha_n^2}\left(\frac{k_1\alpha_n D_n}{\lambda} + \xi_2 A_n\right), \qquad F_n = \frac{\lambda^2}{\alpha_n^2}\left(-\frac{k_2\alpha_n D_n}{\lambda} + \xi_3 A_n\right) \tag{50}$$

For the piezoelastic solution (Solution II), the potential function ϕ representing a general solution to Eq. (25) is given by

$$\phi = \sum_{n=1}^{\infty} J_0(\alpha_n r)\left[B_n\frac{\cosh(\alpha_n z/\mu)}{\sinh(\alpha_n b/\mu)} + C_n\frac{\sinh(\alpha_n z/\mu)}{\cosh(\alpha_n b/\mu)}\right] \tag{51}$$

in which case the solution to Eq. (26) for χ_2 is

$$\chi_2 = \sum_{n=1}^{\infty} \alpha_n^2 J_0(\alpha_n r)\left[B_n\frac{\cosh(\alpha_n z/\mu)}{\sinh(\alpha_n b/\mu)} + C_n\frac{\sinh(\alpha_n z/\mu)}{\cosh(\alpha_n b/\mu)}\right] \tag{52}$$

Here B_n and C_n are arbitrary constants to be determined later through application of the mechanical and electric boundary conditions. Substitution of Eqs. (46)–(52) into Eqs. (9), (11), (14), (21), (23), (24) and (29), and superposition of the results for the two solutions (I and II), yields the following expressions for the displacements, stresses, electric potential and electric displacements induced by T_1:

$$u_r = \sum_{n=1}^{\infty} J_1(\alpha_n r)\left\{ -\alpha_n E_n \frac{\sinh(\alpha_n z/\lambda)}{\sinh(\alpha_n b/\lambda)} + \frac{k_1}{\mu}\alpha_n^2\left[B_n \frac{\sinh(\alpha_n z/\mu)}{\sinh(\alpha_n b/\mu)} + C_n \frac{\cosh(\alpha_n z/\mu)}{\cosh(\alpha_n b/\mu)} \right] \right\} \tag{53}$$

$$u_z = \sum_{n=1}^{\infty} J_0(\alpha_n r)\left\{ \frac{\alpha_n}{\lambda} F_n \frac{\cosh(\alpha_n z/\lambda)}{\sinh(\alpha_n b/\lambda)} - k_2\alpha_n^2\left[B_n \frac{\cosh(\alpha_n z/\mu)}{\sinh(\alpha_n b/\mu)} + C_n \frac{\sinh(\alpha_n z/\mu)}{\cosh(\alpha_n b/\mu)} \right] \right\} \tag{54}$$

$$\begin{aligned}\sigma_{rr} = \sum_{n=1}^{\infty}\Bigg[&\left\{ \left[-c_{11}\alpha_n^2 E_n + \frac{c_{13}\alpha_n^2 F_n}{\lambda^2} + \frac{e_1\alpha_n D_n}{\lambda} - \beta_1 A_n \right] J_0(\alpha_n r) + (c_{11}-c_{12})\alpha_n E_n \frac{J_1(\alpha_n r)}{r} \right\} \\ &\times \frac{\sinh(\alpha_n z/\lambda)}{\sinh(\alpha_n b/\lambda)} + \frac{\alpha_n^2}{\mu}\left\{ (c_{11}k_1 - c_{13}k_2 + e_1)\alpha_n J_0(\alpha_n r) - (c_{11}-c_{12})k_1 \frac{J_1(\alpha_n r)}{r} \right\} \\ &\times \left\{ B_n \frac{\sinh(\alpha_n z/\mu)}{\sinh(\alpha_n b/\mu)} + C_n \frac{\cosh(\alpha_n z/\mu)}{\cosh(\alpha_n b/\mu)} \right\} \Bigg]\end{aligned} \tag{55}$$

$$\begin{aligned}\sigma_{\theta\theta} = \sum_{n=1}^{\infty}\Bigg[&\left\{ \left[-c_{12}\alpha_n^2 E_n + \frac{c_{13}\alpha_n^2 F_n}{\lambda^2} + \frac{e_1\alpha_n D_n}{\lambda} - \beta_1 A_n \right] J_0(\alpha_n r) - (c_{11}-c_{12})\alpha_n E_n \frac{J_1(\alpha_n r)}{r} \right\} \\ &\times \frac{\sinh(\alpha_n z/\lambda)}{\sinh(\alpha_n b/\lambda)} + \frac{\alpha_n^2}{\mu}\left\{ (c_{12}k_1 - c_{13}k_2 + e_1)\alpha_n J_0(\alpha_n r) + (c_{11}-c_{12})k_1 \frac{J_1(\alpha_n r)}{r} \right\} \\ &\times \left\{ B_n \frac{\sinh(\alpha_n z/\mu)}{\sinh(\alpha_n b/\mu)} + C_n \frac{\cosh(\alpha_n z/\mu)}{\cosh(\alpha_n b/\mu)} \right\} \Bigg]\end{aligned} \tag{56}$$

and

$$\Phi = \sum_{n=1}^{\infty} J_0(\alpha_n r)\left\{ D_n \frac{\cosh(\alpha_n z/\lambda)}{\sinh(\alpha_n b/\lambda)} + \alpha_n^2\left[B_n \frac{\cosh(\alpha_n z/\mu)}{\sinh(\alpha_n b/\mu)} + C_n \frac{\sinh(\alpha_n z/\mu)}{\cosh(\alpha_n b/\mu)} \right] \right\} \tag{57}$$

$$D_r = \left(\eta_1 + \frac{e_4^2}{c_{44}} \right) \sum_{n=1}^{\infty} \alpha_n J_1(\alpha_n r)\left\{ D_n \frac{\cosh(\alpha_n z/\lambda)}{\sinh(\alpha_n b/\lambda)} + \alpha_n^2\left[B_n \frac{\cosh(\alpha_n z/\mu)}{\sinh(\alpha_n b/\mu)} + C_n \frac{\sinh(\alpha_n z/\mu)}{\cosh(\alpha_n b/\mu)} \right] \right\} \tag{58}$$

$$\begin{aligned}D_z = \sum_{n=1}^{\infty} J_0(\alpha_n r)\Bigg\{ &\left[-e_1\alpha_n^2 E_n + \frac{e_3\alpha_n^2 F_n}{\lambda^2} - \frac{\eta_3\alpha_n D_n}{\lambda} + p_3 A_n \right] \frac{\sinh(\alpha_n z/\lambda)}{\sinh(\alpha_n b/\lambda)} \\ &+ \frac{\alpha_n^3}{\mu}(e_1k_1 - e_3k_2 - \eta_3)\left[B_n \frac{\sinh(\alpha_n z/\mu)}{\sinh(\alpha_n b/\mu)} + C_n \frac{\cosh(\alpha_n z/\mu)}{\cosh(\alpha_n b/\mu)} \right] \Bigg\}\end{aligned} \tag{59}$$

A simplified expression for σ_{rr} is obtained when Eqs. (47) and (50) for D_n and F_n are substituted into Eq. (55), in which case

$$\sigma_{rr} = \frac{c_{11}-c_{12}}{r} \sum_{n=1}^{\infty} J_1(\alpha_n r)\left[\alpha_n E_n \frac{\sinh(\alpha_n z/\lambda)}{\sinh(\alpha_n b/\lambda)} - \frac{k_1}{\mu}\alpha_n^2 B_n \frac{\sinh(\alpha_n z/\mu)}{\sinh(\alpha_n b/\mu)} \right] \tag{60}$$

The previously undetermined coefficients B_n and C_n are found by applying boundary conditions (38)–(40). Conditions (38) and (39) are found to be satisfied identically, whereas condition (40) leads to the result

$$B_n = \frac{e_1\alpha_n^2 E_n - e_3\alpha_n^2 F_n/\lambda^2 + \eta_3\alpha_n D_n/\lambda - p_3 A_n}{(e_1k_1 - e_3k_2 - \eta_3)\alpha_n^3/\mu}, \quad C_n = 0 \tag{61}$$

Complete expressions for the displacements, stresses, electric potential and electric displacements induced by temperature T then are obtained by summing the respective response quantities associated with T_0 and T_1.

4.2. Case B. Traction-free edge

When the plate is free of traction and electric charge, the relevant boundary conditions are

$$\sigma_{rr} = 0 \quad \text{on } r = a \tag{62}$$

$$D_r = 0 \quad \text{on } r = a \tag{63}$$

$$D_z = 0 \quad \text{on } z = 0, b \tag{64}$$

To obtain the response to the temperature distribution $T_0(z) = A_0(z/b)$, we assume expressions for the displacements and the electric potential of the following forms:

$$u_r = B_0 \frac{rz}{b}, \qquad u_z = -B_0 \frac{r^2}{2b} + C_0 \frac{z^2}{2b} + E_0, \qquad \Phi = D_0 \frac{z^2}{2b} \tag{65}$$

in which B_0, C_0, D_0 and E_0 are constants. The corresponding stresses and electric displacements are

$$\sigma_{rr} = \sigma_{\theta\theta} = [(c_{11} + c_{12})B_0 + c_{13}C_0 + e_1 D_0 - \beta_1 A_0] \frac{z}{b} \tag{66}$$

$$D_r = 0, \qquad D_z = [2e_1 B_0 + e_3 C_0 - \eta_3 D_0 + p_3 A_0] \frac{z}{b} \tag{67}$$

Boundary conditions (62)–(64) require that

$$(c_{11} + c_{12})B_0 + c_{13}C_0 + e_1 D_0 = \beta_1 A_0 \tag{68}$$

and

$$2e_1 B_0 + e_3 C_0 - \eta_3 D_0 = -p_3 A_0 \tag{69}$$

whereas the plane-stress condition $\sigma_{zz} = 0$ implies

$$2c_{13}B_0 + c_{33}C_0 + e_3 D_0 = \beta_3 A_0 \tag{70}$$

Eqs. (68)–(70) are used to compute B_0, C_0 and D_0; constant E_0, which establishes the location of zero transverse displacement, may be selected arbitrarily.

For the response induced by temperature $T_1(r, z)$, the solution derived for Case A (Eqs. (53)–(59)) is applicable here also. Boundary conditions (62)–(64) are satisfied when B_n and C_n are given by Eq. (61). Superposition of response quantities associated with temperatures T_0 and T_1 then leads to the following results:

$$u_r = B_0 \frac{rz}{b} + \sum_{n=1}^{\infty} J_1(\alpha_n r) \left[-\alpha_n E_n \frac{\sinh(\alpha_n z/\lambda)}{\sinh(\alpha_n b/\lambda)} + \frac{k_1}{\mu} \alpha_n^2 B_n \frac{\sinh(\alpha_n z/\mu)}{\sinh(\alpha_n b/\mu)} \right] \tag{71}$$

$$u_z = -B_0 \frac{r^2}{2b} + C_0 \frac{z^2}{2b} + E_0 + \sum_{n=1}^{\infty} J_0(\alpha_n r) \left[\frac{\alpha_n}{\lambda} F_n \frac{\cosh(\alpha_n z/\lambda)}{\sinh(\alpha_n b/\lambda)} - k_2 \alpha_n^2 B_n \frac{\cosh(\alpha_n z/\mu)}{\sinh(\alpha_n b/\mu)} \right] \tag{72}$$

$$\sigma_{rr} = \frac{c_{11} - c_{12}}{r} \sum_{n=1}^{\infty} J_1(\alpha_n r) \left[\alpha_n E_n \frac{\sinh(\alpha_n z/\lambda)}{\sinh(\alpha_n b/\lambda)} - \frac{k_1}{\mu} \alpha_n^2 B_n \frac{\sinh(\alpha_n z/\mu)}{\sinh(\alpha_n b/\mu)} \right] \tag{73}$$

$$\sigma_{\theta\theta} = \sum_{n=1}^{\infty}\left[\left\{\left[-c_{12}\alpha_n^2 E_n + \frac{c_{13}\alpha_n^2 F_n}{\lambda^2} + \frac{e_1\alpha_n D_n}{\lambda} - \beta_1 A_n\right]J_0(\alpha_n r) - (c_{11}-c_{12})\alpha_n E_n \frac{J_1(\alpha_n r)}{r}\right\}\frac{\sinh(\alpha_n z/\lambda)}{\sinh(\alpha_n b/\lambda)} + \frac{\alpha_n^2}{\mu}\left\{(c_{12}k_1 - c_{13}k_2 + e_1)\alpha_n J_0(\alpha_n r) + (c_{11}-c_{12})k_1\frac{J_1(\alpha_n r)}{r}\right\}B_n\frac{\sinh(\alpha_n z/\mu)}{\sinh(\alpha_n b/\mu)}\right] \tag{74}$$

$$\Phi = D_0\frac{z^2}{2b} + \sum_{n=1}^{\infty}J_0(\alpha_n r)\left[D_n\frac{\cosh(\alpha_n z/\lambda)}{\sinh(\alpha_n b/\lambda)} + \alpha_n^2 B_n\frac{\cosh(\alpha_n z/\mu)}{\sinh(\alpha_n b/\mu)}\right] \tag{75}$$

$$D_r = \left(\eta_1 + \frac{e_4^2}{c_{44}}\right)\sum_{n=1}^{\infty}\alpha_n J_1(\alpha_n r)\left[D_n\frac{\cosh(\alpha_n z/\lambda)}{\sinh(\alpha_n b/\lambda)} + \alpha_n^2 B_n\frac{\cosh(\alpha_n z/\mu)}{\sinh(\alpha_n b/\mu)}\right] \tag{76}$$

$$D_z = \sum_{n=1}^{\infty}J_0(\alpha_n r)\left[\left(-e_1\alpha_n^2 E_n + \frac{e_3\alpha_n^2 F_n}{\lambda^2} - \frac{\eta_3\alpha_n D_n}{\lambda} + p_3 A_n\right)\frac{\sinh(\alpha_n z/\lambda)}{\sinh(\alpha_n b/\lambda)} + \frac{\alpha_n^3}{\mu}(e_1k_1 - e_3k_2 - \eta_3)B_n\frac{\sinh(\alpha_n z/\mu)}{\sinh(\alpha_n b/\mu)}\right] \tag{77}$$

5. Numerical results

As an illustrative example, the ambient temperature $Q(r)$ on the face $z = b$ of the plate is taken to have a radial distribution described by

$$Q(r) = T_0\left(1 - 2\frac{r^2}{a^2} + \frac{r^4}{a^4}\right) \tag{78}$$

The plate material is considered to be cadmium selenide, having the following properties (Berlincourt et al., 1963):

$$\begin{aligned}
&c_{11} = 74.1\times10^9\ \mathrm{N\,m^{-2}}, \quad c_{12} = 45.2\times10^9\ \mathrm{N\,m^{-2}}, \quad c_{13} = 39.3\times10^9\ \mathrm{N\,m^{-2}},\\
&c_{33} = 83.6\times10^9\ \mathrm{N\,m^{-2}}, \quad c_{44} = 13.2\times10^9\ \mathrm{N\,m^{-2}},\\
&\beta_1 = 0.621\times10^6\ \mathrm{N\,K^{-1}\,m^{-2}}, \quad \beta_3 = 0.551\times10^6\ \mathrm{N\,K^{-1}\,m^{-2}},\\
&e_1 = -0.160\ \mathrm{C\,m^{-2}}, \quad e_3 = 0.347\ \mathrm{C\,m^{-2}}, \quad e_4 = -0.138\ \mathrm{C\,m^{-2}},\\
&\eta_1 = 82.6\times10^{-12}\ \mathrm{C^2\,N^{-1}\,m^{-2}}, \quad \eta_3 = 90.3\times10^{-12}\ \mathrm{C^2\,N^{-1}\,m^{-2}}, \quad p_3 = -2.94\times10^{-6}\ \mathrm{C\,K^{-1}\,m^{-2}},\\
&\lambda_r = \lambda_z = 9\ \mathrm{W\,K^{-1}\,m^{-1}}, \quad \alpha_r = 4.4\times10^{-6}\ \mathrm{K^{-1}},\\
&Y_r = 42.8\times10^9\ \mathrm{N\,m^{-2}}, \quad G_{rz} = 13.2\times10^9\ \mathrm{N\,m^{-2}}, \quad v_{r\theta} = 0.480, \quad v_{rz} = 0.245,
\end{aligned} \tag{79}$$

where, in addition to quantities defined earlier, α_r, Y_r, G_{rz}, $v_{r\theta}$ and v_{rz} denote, respectively, thermal expansion coefficient, Young's modulus, shear modulus and Poisson ratios.

The following dimensionless quantities are introduced for convenience in the presentation of numerical results:

$$\begin{aligned}
&\overline{b}=\frac{b}{a}, \qquad \overline{r}=\frac{r}{a}, \qquad \overline{z}=\frac{z}{a}, \qquad B=ah, \qquad \overline{T}=\frac{T}{T_0},\\
&\overline{u}_i=\frac{u_i}{a\alpha_r T_0}, \qquad \overline{\sigma}_{ij}=\frac{\sigma_{ij}}{\alpha_r Y_r T_0}, \qquad \overline{\Phi}=\sqrt{\frac{\eta_1}{Y_r}}\frac{\Phi}{a\alpha_r T_0}, \qquad \overline{D}_i=\frac{D_i}{\sqrt{Y_r\eta_1}\alpha_r T_0},\\
&\overline{\lambda}^2=\frac{\lambda_z}{\lambda_r}, \qquad \overline{\alpha}=\frac{\alpha_z}{\alpha_r}, \qquad \overline{Y}=\frac{Y_z}{Y_r}, \qquad \overline{G}=\frac{G_{rz}}{Y_r},\\
&\overline{e}_i=\frac{e_i}{\sqrt{Y_r\eta_1}}, \qquad \overline{\eta}=\frac{\eta_3}{\eta_1}, \qquad \overline{p}_3=\frac{p_3}{\sqrt{Y_r\eta_1}\alpha_r}.
\end{aligned} \tag{80}$$

Results obtained using the present formulation for a plate having a radially-constrained edge (Case A) were found to be in complete agreement with those computed using the solution procedure given earlier (Ashida and Tauchert, 2000). As previously noted, the earlier formulation was limited to plates having a constrained cylindrical edge. Since results for that case were provided in the earlier paper, only results for the traction-free plate (Case B) are reported here. All response quantities have been calculated by retaining the first 50 terms in the corresponding infinite series.

Fig. 1 shows the radial variation of the nondimensionalized surface temperature $[\overline{T}]_{\overline{z}=\overline{b}}$ for plates of various thickness-to-radius ratios $\overline{b}$, in the case of Biot number $B_i = 1$. The corresponding distributions of radial displacement, transverse displacement difference between the plate surfaces, radial and circumferential stresses, electric potential difference, and radial electric displacements, are given in Figs. 2–6, respectively. The maximum (absolute) value of each response quantity increases with increasing plate thickness. Maximum values of surface temperature, transverse displacement difference, radial and circumferential stresses, and

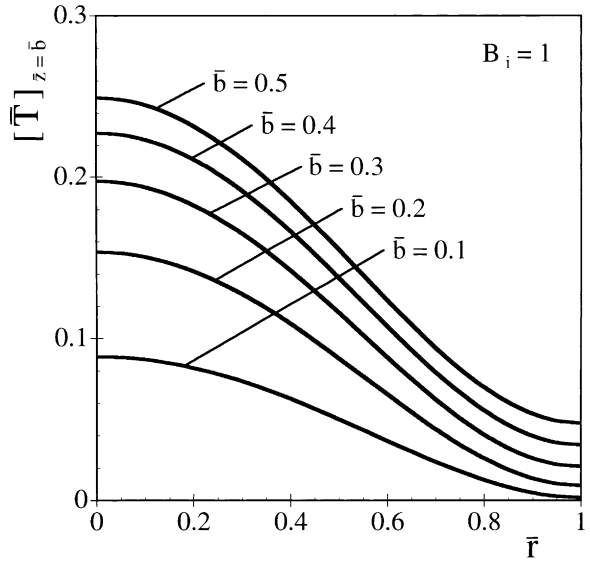

Fig. 1. Distributions of surface temperature for different values of thickness-to-radius ratio $\overline{b}$.

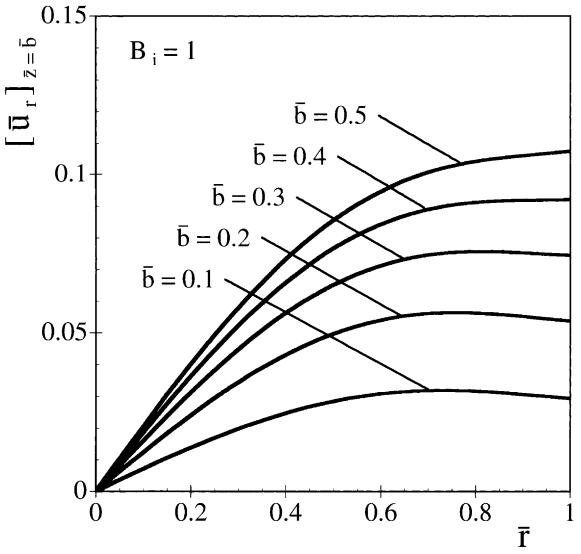

Fig. 2. Distributions of radial displacement for different values of thickness-to-radius ratio $\bar{b}$.

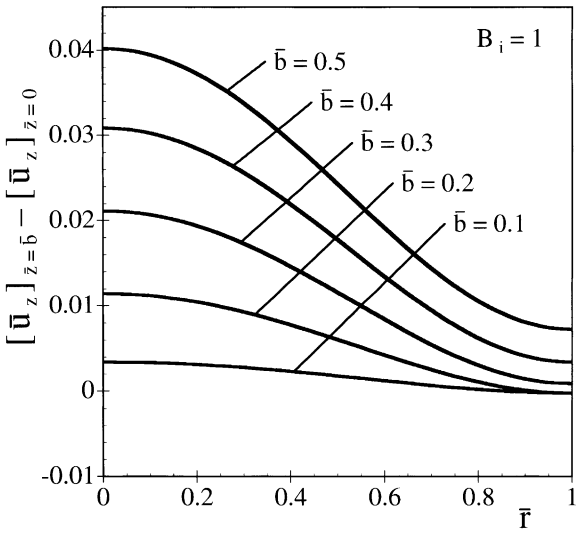

Fig. 3. Distributions of transverse displacement difference between the plate surfaces for different values of thickness-to-radius ratio $\bar{b}$.

electric potential difference occur at the center of the plate; the radial displacement is maximum at the plate edge; radial electric displacements at the plate surfaces are greatest at approximately $\bar{r} = 0.52$.

Figs. 7–9 illustrate the effects of variations in material properties on the stresses at the center of the heated surface of the plate. The plate considered in this case has a thickness-to-radius ratio $\bar{b} = 0.2$, and the Biot number is $B_i = 1$. A parameter γ $(0.01 \leqslant \gamma \leqslant 100)$ is applied to a particular material property to illustrate the effect of varying that property when all other properties have the values given in Eq. (80). The

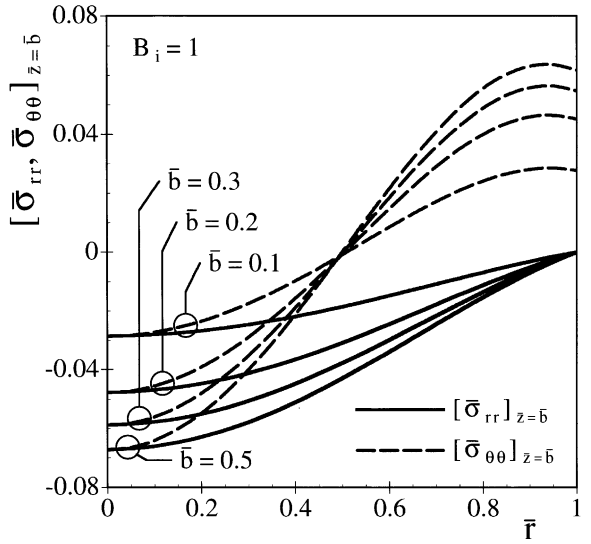

Fig. 4. Distributions of radial and circumferential stresses for different values of thickness-to-radius ratio $\bar{b}$.

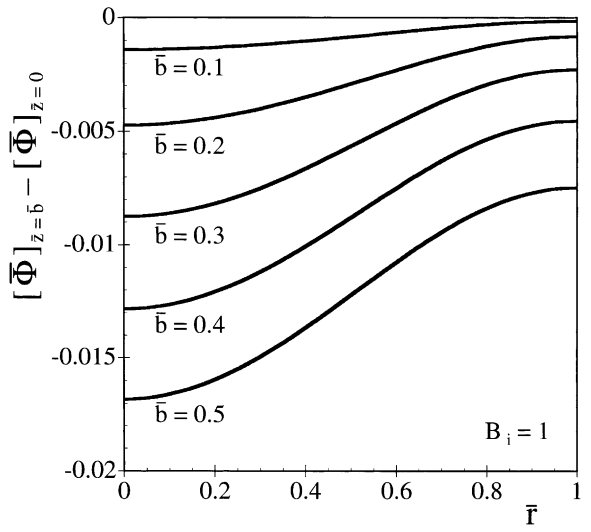

Fig. 5. Distributions of electric potential difference between the plate surfaces for different values of thickness-to-radius ratio $\bar{b}$.

effects of having different dimensionless values of thermal expansion coefficient $\bar{\alpha}$, thermal conductivity ratio $\bar{\lambda}^2$, and pyroelectric coefficient $\bar{p}_3$ are shown in Fig. 7. Fig. 8 shows the influence of different Poisson ratios $v_{r\theta}$ and v_{rz} over the range $(\gamma v_{r\theta}, \gamma v_{rz}) \leqslant 0.5$, shear modulus variation over the range $\gamma \bar{G} \leqslant 0.5$, and variation of Young's modulus ratio $\bar{Y}$. The effects of differences in dielectric permittivity $\bar{\eta}$ and piezoelectric coefficients $\bar{e}_1$, $\bar{e}_3$ and $\bar{e}_4$ are shown in Fig. 9. It can be seen that the stress amplitudes are affected significantly by $\bar{\alpha}$, $\bar{\lambda}^2$, $\bar{p}_3$, $\bar{\eta}$, $\bar{e}_1$ and $\bar{e}_3$, but are relatively less sensitive to variations in $v_{r\theta}$, v_{rz}, $\bar{G}$, $\bar{Y}$ and $\bar{e}_4$ over the range of γ considered.

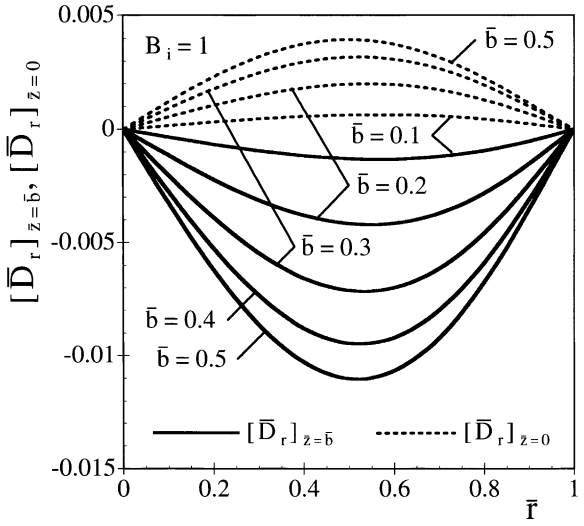

Fig. 6. Distributions of radial electric displacement for different values of thickness-to-radius ratio $\bar{b}$.

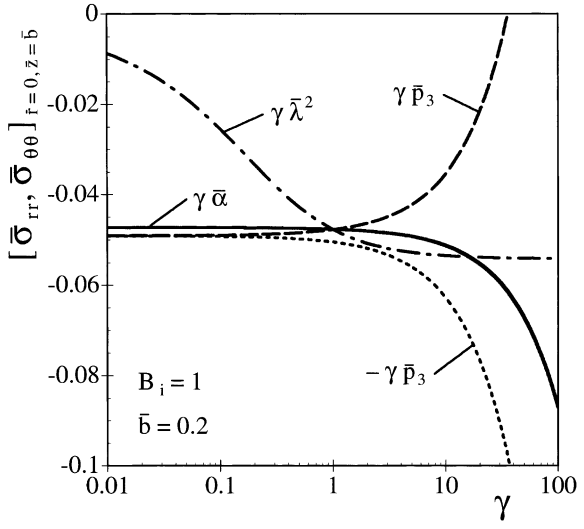

Fig. 7. Effect of variations in material properties $\bar{\alpha}$, $\bar{\lambda}^2$ and $\bar{p}_3$ upon stresses.

Figs. 10–12 illustrate the effects of variations of these same material properties on the difference in electric potential between the plate surfaces. Note that the amplitude of the potential difference is particularly sensitive to variations in $\bar{\alpha}$, $\bar{p}_3$ and $\bar{\eta}$, but relatively insensitive to variations in the other properties.

6. Concluding remarks

The plane-stress piezothermoelastic formulation presented here is more general than the authors' earlier formulation (2000), in that it is applicable in the case of traction-free as well as constrained edge

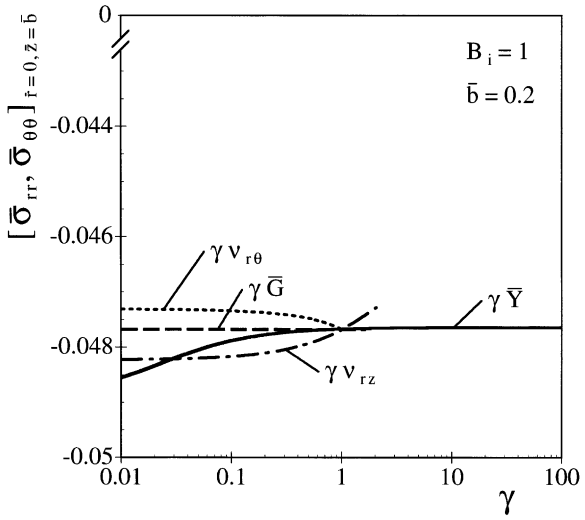

Fig. 8. Effect of variations in material properties $v_{r\theta}$, v_{rz}, $\overline{G}$ and $\overline{Y}$ upon stresses.

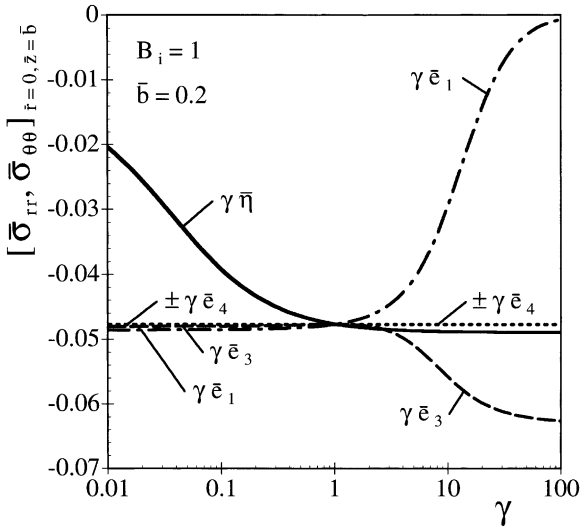

Fig. 9. Effect of variations in material properties $\bar{e}_1$, $\bar{e}_3$, $\bar{e}_4$ and $\bar{\eta}$ upon stresses.

conditions. Results for the radially constrained plate are in complete agreement with those presented earlier.

From a computational viewpoint, application of the plane-stress solution is far simpler than that of the three-dimensional solution procedure developed by Ashida and Tauchert (1998). As indicated in the author's previous study (2000), the plane-stress approximation generally yields results that are in good agreement with the corresponding exact three-dimensional solution, even in the case of plates with thickness equal to the radius.

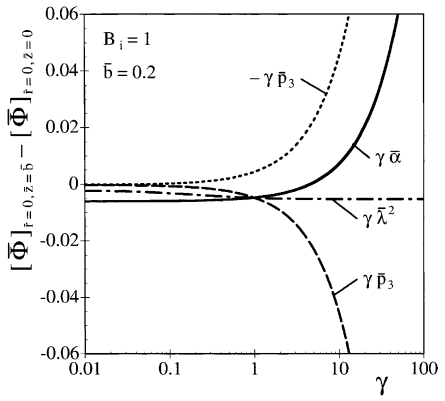

Fig. 10. Effect of variations in material properties $\bar{\alpha}$, $\bar{\lambda}^2$ and $\bar{p}_3$ upon electric potential difference between the plate surfaces.

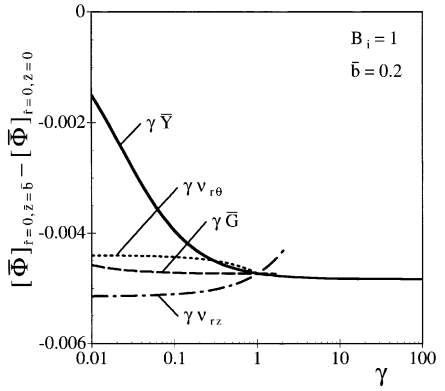

Fig. 11. Effect of variations in material properties $v_{r\theta}$, v_{rz}, $\overline{G}$ and $\overline{Y}$ upon electric potential difference between the plate surfaces.

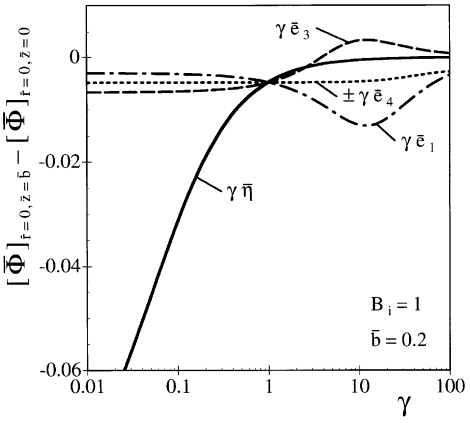

Fig. 12. Effect of variations in material properties $\bar{e}_1$, $\bar{e}_3$, $\bar{e}_4$ and $\bar{\eta}$ upon electric potential difference between the plate surfaces.

References

Ashida, F., Tauchert, T.R., 1998. Transient response of a piezothermoelastic circular disk under axisymmetric heating. Acta Mech. 128, 1–14.

Ashida, F., Tauchert, T.R., 2000. Plane stress problem of a piezothermoelastic plate. Acta Mech., submitted for publication.

Berlincourt, D., Jaffe, H., Shiozawa, L.R., 1963. Electroelastic properties of the sulfides, selenides, and tellurides of zinc and cadmium. Phys. Rev. 129, 1009–1017.

Chandrashekhara, K., Agarwal, A.N., 1993. Active vibration control of laminated composite plates using piezoelectric devices: a finite element approach. J. Intelligent Mater. Sys. Struct. 4, 496–508.

Dube, G.P., Kapuria, S., Dumir, P.C., 1996. Exact piezothermoelastic solution of simply-supported orthotropic flat panel in cylindrical bending. Int. J. Mech. Sci. 38, 1161–1177.

Heyliger, P., 1994. Static behavior of laminated elastic/piezoelectric plates. AIAA J. 32, 2481–2484.

Jonnalagadda, K.D., Blandford, G.E., Tauchert, T.R., 1994. Piezothermoelastic composite plate analysis using first-order shear deformation theory. Comput. Struct. 51, 79–89.

Kapuria, S., Dumir, P.C., Segupta, S., 1998. Three-dimensional axisymmetric piezothermoelastic solution of a transversely isotropic piezoelectric clamped circular plate. J. Appl. Mech. 65, 178–183.

Lee, C.K., 1990. Theory of laminated piezoelectric plates for the design of distributed sensors/actuators: part I: governing equations and reciprocal relationships. J. Acoust. Soc. Amer. 87, 1144–1158.

Mindlin, R.D., 1961. On the equations of motion of piezoelectric crystals. Problems of Continuum Mechanics, Muskhelishvili, N.I., 70th birthday volume, pp. 282–290.

Mitchell, J.A., Reddy, J.N., 1995. A refined hybrid plate theory for composite laminates with piezoelectric laminae. Int. J. Solids Struct. 32, 2345–2367.

Noda, N., Kimura, S., 1998. Deformation of a piezothermoelectric composite plate considering the coupling effect. J. Thermal Stresses 21, 359–379.

Ray, M.C., Bhattacharya, R., Samanta, B., 1993a. Static analysis of an intelligent structure by the finite element method. Comput. Struct. 52, 617–631.

Ray, M.C., Bhattacharya, R., Samanta, B., 1993b. Exact solutions for static analysis of intelligent structures. AIAA J. 31, 1684–1691.

Reddy, J.N., 1996. Refined theories and computational procedures for the modeling of smart composite structures. Proc. 1st Int. Conf. Compos. Sci. Technol., pp. 421–429.

Saravanos, D.A., Heyliger, P.R., Hopkins, D.A., 1997. Layerwise mechanics and finite element model for the dynamic analysis of piezoelectric composite plates. Int. J. Solids Struct. 34, 359–378.

Tang, Y.Y., Noor, A.K., Xu, K., 1996. Assessment of computational models for thermoelectroelastic multilayered plates. Comput. Struct. 61, 915–933.

Tauchert, T.R., 1992. Piezothermoelastic behavior of a laminated plate. J. Thermal Stresses 15, 25–37.

Tauchert, T.R., Ashida, F., Noda, N., Adali, S., Verijenko, V., 2000. Developments in thermopiezoelasticity with relevance to smart composite structures. Compos. Struct. 48, 31–38.

Tiersten, H.F., 1971. On the nonlinear equations of thermoelectroelasticity. Int. J. Engng. Sci. 9, 587–604.

Xu, K., Noor, A.K., Tang, Y.Y., 1995. Three-dimensional solutions for coupled thermoelectroelastic response of multilayered plates. Comput. Meth. Appl. Mech. Engng. 126, 355–371.